Journal of Power Sources 214 (2012) 15–20

Contents lists available at SciVerse ScienceDirect

Journal of Power Sources

journal homepage: www.elsevier.com/locate/jpowsour

Highly active non-precious metal catalyst based on poly(vinylpyrrolidone)–wrapped carbon nanotubes complexed with iron–cobalt metal ions for oxygen reduction reaction

San Hua Lim*, Zitai Li, Chee Kok Poh, Linfei Lai, Jianyi Lin

*Institute of Chemical and Engineering Sciences, A*STAR, 1 Pesek Road, Jurong Island 627833, Singapore*

ARTICLE INFO

Article history:
Received 16 January 2012
Received in revised form
23 March 2012
Accepted 25 March 2012
Available online 21 April 2012

Keywords:
Carbon nanotube
Fuel cell
Oxygen reduction
Bimetallic
Catalysts

ABSTRACT

Multi-walled carbon nanotubes (MWCNTs) are functionalized with 2-pyrridone functional groups by wrapping poly(vinylpyrrolidone) polymers around it under high-powered sonication. The presence of 2-pyrridone functional groups facilitates the complexation of metal ions (Fe^{3+}, Co^{2+}). The best oxygen reduction catalyst, MWCNT–FeCo, is synthesized by annealing poly(vinylpyrrolidone)/MWCNTs/Fe–Co complex in ammonia at 900 °C and exhibits nearly four-electron oxygen pathway (n ~3.8). X-ray diffraction pattern shows that low loading of metallic Fe nanoparticles (0.79 wt.%) and bimetallic FeCo nanoparticles (0.34 wt.%) is formed on the MWCNT–FeCo catalysts. X-ray photoelectron spectroscopy reveals that ~1 at.% of nitrogen has been doped into MWCNT–FeCo catalysts.

1. Introduction

Polymer electrolyte membrane fuel cell (PEMFC) is a very promising energy converting device with high efficiency, scalability and low carbon emission [1–3]. PEMFC relies on hydrogen and oxygen (or air) as feedstocks which are renewable and sustainable. PEMFC has a wide range of potential applications such as on-board transportation, portable devices and stationary power station [1–3]. However the high material costs deter the commercialization of PEMFC. Particularly the fuel cell performance relies on expensive and precious platinum catalysts, which account for ~40% of its material costs. As a short term solution, the utilization of suitable carbon supports and improvement of synthesis method help to reduce Pt loading. For example, Matsumoto et al. [4] reported that Pt catalysts supported on multi-walled carbon nanotubes (MWCNTs) not only significantly reduced the Pt loading by 60% but also improved the fuel cell performance voltages by 10%.

The chemical reactions of a PEMFC involve Pt nanoparticles catalyzing a hydrogen oxidation reaction (HOR) at the anode, and an oxygen reduction reaction (ORR) at the cathode. In comparison, HOR has a smaller overpotential of <25 mV, while ORR has a larger overpotential of ≫300 mV for a moderate current density less than 1 A cm^{-2} [5]. The slow kinetics of ORR at the cathode often hampers the fuel cell overall performance. The development of low cost, non-precious and high performance oxygen electrocatalysts as alternatives for Pt will be a great incentive for the commercialization of PEMFCs. Taking Pt catalyst as a benchmark, these new and non-precious metal catalysts (NPMCs) should ideally catalyze ORR via four-electron pathway with low overpotential, low H_2O_2 production, and better tolerance of contaminants.

A number of materials have been investigated as NPMCs which include transition metal oxides, carbides, nitrides, oxynitrides, metal chalcogenides, and pyrolyzed macrocyclic molecules [6–9]. Among these materials, pyrolyzed macrocyclic molecules with N_4-chelates (e.g. Fe and Co phthalocynine, porphyrins and tetraazannulenes) have been widely studied and shown very promising ORR catalytic activity [10–21]. The end products of pyrolyzed macrocyclic molecules usually consist of nitrogen-enriched carbonaceous materials with transition metal dopants, which are stable in the acidic environment of PEMFC. However, macrocyclic compounds are expensive and insights from the study of pyrolyzed macrocyclic molecules reveal that the N_4-chelates eventually decompose into metal–nitrogen–carbon fragments, and NPMCs can also be prepared from cheaper precursors. A generic method of synthesizing NMPC involves mixing nitrogen-rich precursors (e.g. polyaniline, polypyrrole or ethylenediamine), salts of Fe/Co and

* Corresponding author. Tel.: +65 6796 3828; fax: +65 6316 6182.
E-mail address: lim_san_hua@ices.a-star.edu.sg (S.H. Lim).

0378-7753/$ – see front matter © 2012 Elsevier B.V. All rights reserved.
doi:10.1016/j.jpowsour.2012.03.094

carbon supports together, and then annealing the mixture in ammonia at 600–1000 °C. Current research posits the metal–nitrogen–carbon sites as catalytic centers for the ORR activity, though the exact nature of the catalytic sites is still under debate. Dodelet and co-workers [12] synthesized Fe-based NPMCs, and proposed that the Fe ions in the center of the sites of Fe–N_4–C (pyrrolic nitrogen) and Fe–N_2–C (pyridinic-nitrogen) act as catalytic sites for ORR. Nabae et al. [10] studied the role of Fe species in the pyrolysis of Fe phthalocyanine for the synthesis of NPMCs. NMPCs based on Fe phthalocyanine exhibit the best ORR activity when it is pyrolyzed at 600 °C. The N_4-chelates are partially decomposed into Fe–nitrile complexes at ~400–550 °C. As the temperature is increased to 600 °C, the Fe species convert from mononuclear form to Fe nanoparticles and yield nitrogen-enriched carbon solids. However at >700 °C, the Fe nanoparticles start to displace more N dopants from the carbon solids and result in lower nitrogen concentration. Similarly, Yuasa et al. [14] synthesized NPMCs consisting of carbon/polypyrrole/Co ions composites with tetrapyrrole-type coordination sites. On the basis of surface science analysis, Yuasa et al. [14] showed that the carbon/polypyrrole/cobalt ions NPMC pyrolyzed at 550–600 °C exhibited a Co–N_4 structure, while metallic Co nanoparticles were formed at higher temperatures. However the maximum ORR activity of carbon/polypyrrole/cobalt ions NPMCs was observed near 700 °C.

Although iron and cobalt metal complexes were used separately to synthesize nitrogen-doped carbons, the study of bimetallic FeCo nanoparticles to synthesized nitrogen-doped carbons and its effects on the ORR activity was rather limited. Therefore it will be of great interests to investigate the synergistic effects of bimetallic FeCo nanoparticles to synthesized nitrogen-doped carbon-based ORR catalysts.

In this manuscript, the application of poly(vinylpyrrolidone)-wrapped MWCNTs complexed with Fe and/or Co metal ions was used for the synthesis of metal–nitrogen–carbon NPMCs. MWCNTs have been extensively studied as carbon supports for anode in PEMFC, and thus it should also be good supports for cathode. Although the wrapping action of PVP around carbon nanotube has already been reported in literature [22], but there is no report on the application of these PVP–wrapped nanotube composites. To the best of our knowledge, the application of poly(vinylpyrrolidone)-wrapped MWCNTs for the preparation of oxygen reduction reaction catalysts has not been reported in literature. Nitrogen-doped MWCNTs are easily synthesized from annealing poly(vinylpyrrolidone)-wrapped MWCNTs in ammonia. The best NPMC for ORR activity was synthesized from PVP–wrapped MWCNTs complexed with Fe–Co ions.

2. Experimental

Multi-walled carbon nanotubes (MWCNTs) with 10–20 nm diameters were purchased from Shenzhen Nanotech Port Co., Ltd, China. Poly(vinylpyrrolidone) with average molecular weight of 10,000, iron (III) chloride hexahydrate (ACS reagent, 97%) and cobalt (II) acetate tetrahydrate (ACS reagent, ≥98%) were purchased from Sigma–Aldrich. Commercially available platinum catalysts (20 wt.%) supported on Black Pearl 2000 (BP2K-20%Pt) were purchased from E-TEK. All the chemicals were used as received. 500 mg of MWCNTs and 250 mg of PVP were mixed together in water and ultrasonicated at 150 W for 30 min. A very stable dispersion of MWCNT–PVP composites was obtained after ultrasonication. A metal loading (Fe or Co) of 2 wt.% was added to the stable dispersion of MWCNT–PVP. For bimetallic FeCo, a loading of 1 wt.% of each constituent was added to the MWCNT–PVP composites. After 1 h of stirring, the excess water was removed by evaporation. The MWCNT–PVP–metal ion complexes were annealed in 10% NH_3 at 900 °C for 1 h. The schematic diagram for the synthesis of Fe/Co–N–C NPMCs for oxygen reduction reaction based on PVP–wrapped MWCNTs was shown in Fig. 1.

The as-prepared catalysts were characterized by X-ray powder diffraction (XRD, Bruker D8 Advance) using Cu Kα radiation ($\lambda = 0.154$ nm). The morphology of the samples was studied using a scanning electron microscope (SEM, JEOL JSM-6700F) coupled with an energy dispersive X-ray detector (EDX, Oxford

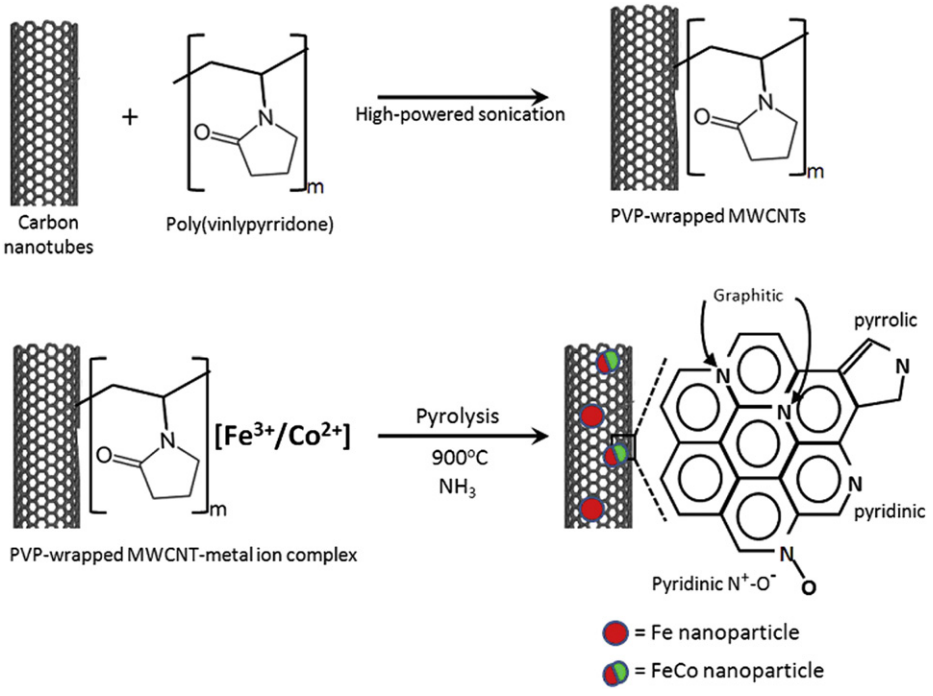

Fig. 1. Schematic diagram for the conversion of poly(vinylpyrrolidone)–wrapped-multi-walled carbon nanotubes into Fe/Co–N–C catalysts.

Instruments). The catalysts were mounted onto copper tapes for SEM and EDX analysis. The copper Kα lines were used for 'Quant Optimization' and to calibrate the EDX detector. On the basis of EDX analysis, the weight percentage of elemental Fe and Co contents was determined with respect to the carbon content. The chemical bonding of the samples was studied using X-ray photoelectron spectroscopy (XPS, ESCALAB-250 Thermo VG Scientific), and a monochromatic Al Kα ($h\nu = 1486.6$ eV) excitation was employed. The N1s peaks were fitted using a mixed 80% Gaussian–20% Lorentzian shaped profile with a linear background. Identical fitting parameters with 2 eV full width at half maximum (FWHM) were used for all the measured N1s peaks. The specific surface area and pore volume of the PVP–wrapped MWCNT-based NPMCs were analyzed and determined on Micromeritics BET analyzer (ASAP 2420), using the Brunauer, Emmett and Teller theory (BET), Barrett–Joyner–Halenda (BJH) equations and the adsorption data.

All the electrochemical measurements were carried out using AutoLab electrochemical workstation (AT302). The working electrode was fabricated by casting a Nafion-impregnated catalyst ink onto a glassy carbon electrode (3 mm in diameter). Typically, 10 mg of the MWCNT catalysts were mixed in 2 ml of ethanol aqueous solution (1:1 v/v). To form the catalyst ink, 60 μl of a 5 wt% Nafion

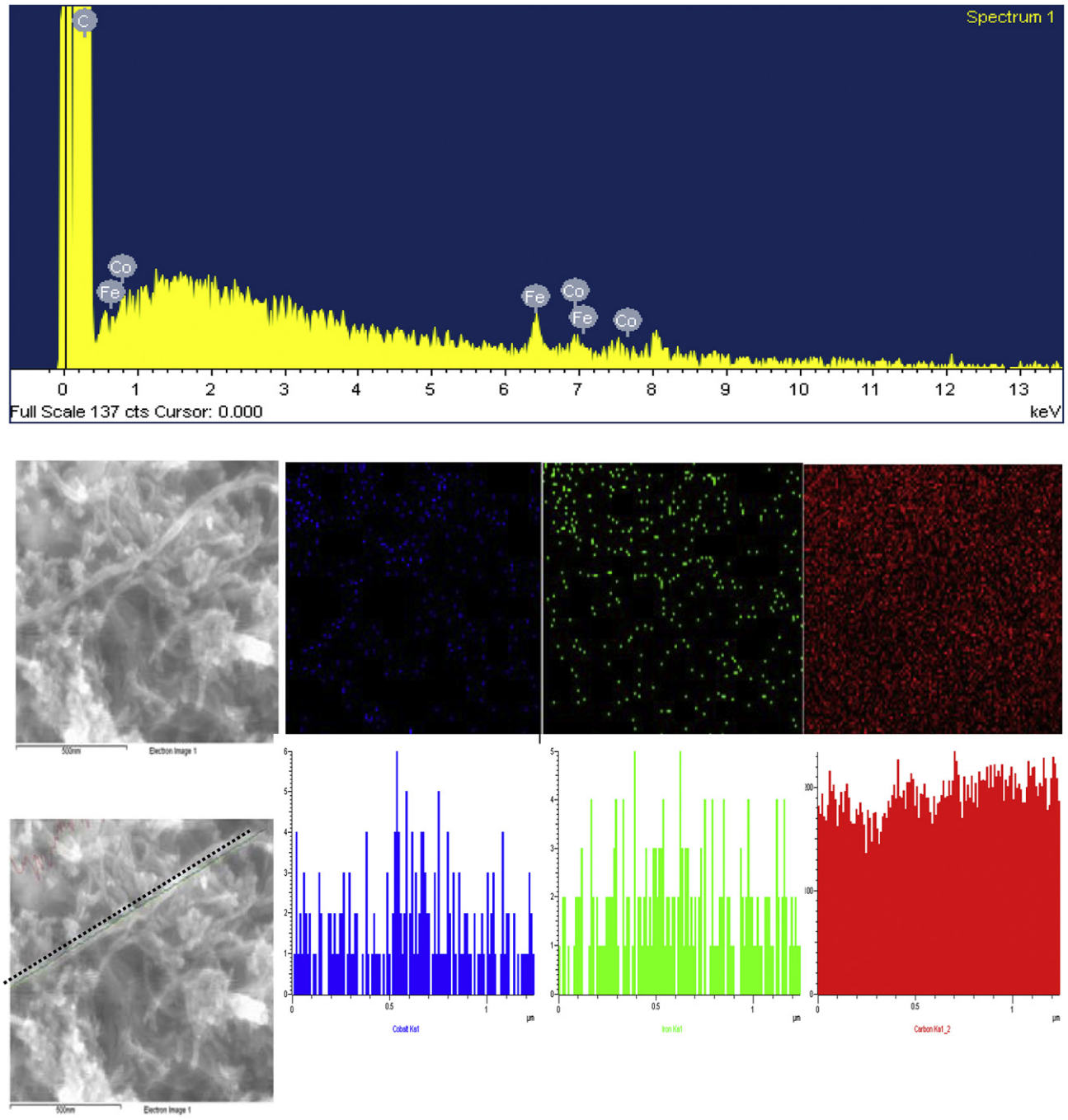

Fig. 2. Scanning electron microscopic (SEM) images, energy dispersive X-ray (EDX) analysis and elemental mapping and line scan of MWCNT–FeCo catalysts. The elemental mapping of cobalt, iron and carbon are denoted as blue, green and red colors respectively. Unlabeled peaks are due to the Cu Kα signals from the copper tape. (For interpretation of the references to color in this figure legend, the reader is referred to the web version of this article.)

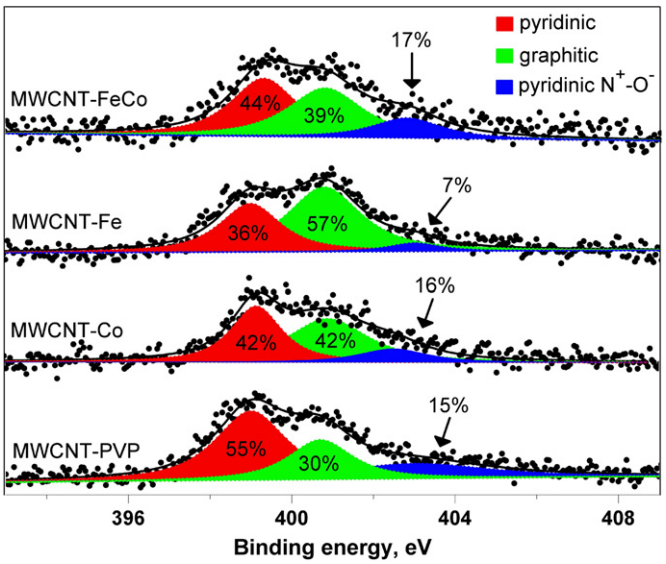

Fig. 3. X-ray photoelectron spectroscopy (XPS) core-level N1s spectra of various non-precious metal–carbon nanotube-based catalysts.

solution (as binder) was added to the MWCNT catalysts and sonicated for 15 min. 10 μl of this catalyst ink was drop-cast onto the glassy carbon electrode. The electrode was dried in an oven at 70 °C. For rotating disk electrode (RDE) measurements the working electrode was immersed in 0.5 M H_2SO_4 acid, which was purged with oxygen/argon gas for linear voltammetry measurements. A Pt foil and an Ag/AgCl (3 M) electrode were used as counter electrode and reference electrode, respectively. The ORR curves were recorded from +1.0 to −0.2 V potential at a scan rate of 10 mV s^{-1}. The rotation rate of the modified glass carbon electrodes was varied from 250 to 4000 rpm.

3. Results and discussion

As schematically shown in Fig. 1, NPMCs supported on PVP–wrapped MWCNTs were synthesized by pyrolysis of FeCo–poly(vinylpyrridone)–MWCNTs composites.

The SEM image and the energy dispersive X-ray (EDX) analysis of the pyrolyzed MWCNT–FeCo catalysts were presented in Fig. 2. Elemental (iron, cobalt and carbon) mapping and line scan (1.2 μm in length along an individual MWCNT–FeCo) both demonstrate that Fe and Co elements are well-distributed along the nanotube. The total metallic loadings of the non-precious metal (Fe and Co) in the pyrolyzed FeCo–carbon nanotube catalysts are about 1 wt.%.

The application of PVP polymer and ammonia annealing provides a very simple and cost-effective method to convert pristine MWCNTs into nitrogen-doped carbon nanotubes. PVP is a water soluble polymer which has excellent wetting properties and readily binds to polar molecules. It has been widely used in coating and colloid chemistry to form films or to stabilize metal particles, forming pyrridone–metal ion complexes [23–25]. The wrapping of MWCNTs with PVP instantly functionalized the nanotubes with 2-pyrridone functional groups and avoids lengthy and damaging acid functionalization. In comparison to wet impregnation method, the utilization of PVP–wrapped MWCNTs as the catalyst support ensures the uniform distribution of transition metal ions (Fe and Co ions). In the absence of transition metal ions, PVP–wrapped MWNCNTs are easily converted to nitrogen-doped carbon nanotubes. In the presence of metal salts Fe^{3+} and Co^{2+} can be readily chemisorbed onto the 2-pyrridone functional groups, due to the high polarity of the near-planer lactam ring [25]. The pyrridone–metal ion complexes are anchored on the exteriors of carbon nanotubes. Annealing of the MWCNT–PVP–metal ion complexes in 10% NH_3 atmosphere at 900 °C for 1 h yields the good ORR catalysts in which the active sites are easily accessible for oxygen reduction reaction.

The nature of nitrogenation in these non-precious metal–carbon nanotube-based catalysts was studied using XPS technique. Several nitrogen species are commonly reported in literature for pyrolyzed nitrogen-doped carbon compounds [26]. These include: (1) graphitic-nitrogen (401.3 ± 0.3 eV) in which the nitrogen is within the graphite plane and bond to three carbon atoms, and (2) pyridinic-nitrogen (398.6 ± 0.3 eV) which is located on the edge of graphite planes and bond to two carbon atoms. (3) Pyrrolic nitrogen which is sp^3-coordinated in five-member rings of the carbon sheet and is often assigned to peaks at 400.5 ± 0.3 eV. (4) A pyridinic-N^+–O^- species with a high binding energy ~402–405 eV which are ascribed as oxidized protonated pyridyl functional groups when the samples are exposed to air. Detailed XPS studies of the evolution of nitrogen functionalities of carbonaceous materials during pyrolysis revealed that pyrrolic nitrogen decompose to pyridinic-N and graphitic-N above 600 °C [26]. Hence for the catalysts annealed at 900 °C, the pyrrolic nitrogen was not used in the core-level N1s peak deconvolution and the N1s peaks of the catalysts were deconvoluted into 3 major components of graphitic, pyridinic and pyridinic-N^+–O^- species. As presented in Fig. 3 and Table 1, PVP–wrapped MWCNTs were converted to N-doped MWCNTs (1.5 at.% of nitrogen) after annealing in 10% NH_3 at 900 °C. When metal catalysts were loaded to the MWCNT–PVP, the amount of nitrogen dopants was reduced to ~1 at.%. The types of N species formed in MWCNT–PVP are approximately 30% graphitic, 55% pyridinic and 15% pyridinic-N^+–O^- species. The MWCNT–Fe catalysts exhibit a higher amount of graphitic-nitrogen (~57%) and lower amount of pyridinic (~36%) and pyridinic-N^+–O^- species (~7%) compared to the MWCNT–PVP catalysts. The MWCNT–Co catalysts show ~42% of graphitic and pyridinic-nitrogen and ~16% of pyridinic-N^+–O^- species. The MWCNT–FeCo catalysts show ~39% of graphitic-nitrogen, ~44% pyridinic and ~17% pyridinic-N^+–O^- species. The XRD patterns of the as-

Table 1
Physical properties, EDX elemental analysis and relative concentration of nitrogen species of non-precious metal–carbon nanotube catalysts.

Sample	Specific surface area and pore volume		EDX elemental analysis (wt%)			XPS core-level N1s peak fitting		
	BET S.A. ($m^2\ g^{-1}$)	BJH pore volume ($cm^3\ g^{-1}$)	Fe	Co	Total N content (at%)	Graphitic (%)	Pyridinic (%)	N^+-O^- (%)
MWCNT	138	0.72	–	–	–	–	–	–
MWCNT–PVP	127	0.65	–	–	1.5	30	55	15
MWCNT–Fe	110	0.38	1.05	–	1.4	57	36	7
MWCNT–Co	115	0.45	–	1.03	1.0	42	42	16
MWCNT–FeCo	112	0.61	0.79	0.34	1.0	39	44	17

prepared catalysts were displayed in Fig. 4. The metallic states of Fe (JCPDS 6-0696) and Co nanoparticles (JCPDS 15-0806) are detected in the MWCNT–Fe and MWCNT–Co samples respectively. It is interesting that both Fe nanoparticles and bimetallic FeCo alloys (JCPDS 49-1568) are present in MWCNT–FeCo samples. The metallic nanoparticles displace nitrogen dopants from carbon solids at >700 °C [10]. On the basis of XPS and XRD analysis, the types of metallic nanoparticles have a significant influence on the nature of nitrogen dopants. Fe nanoparticles favor the formation of graphitic-nitrogen, while Co nanoparticles favor the formation of pyridinic-nitrogen and protonated pyridyl moiety. Thus the role of the metal nanoparticles plays an important role in defining the nature of the N species produced in the carbon nanotubes in the doping process. In addition, the MWCNT–FeCo catalysts were pickled in 0.5 M H_2SO_4 acid under vigorous stirring for 24 h at room temperature to test the stability of the metal nanoparticles in an acidic electrolyte. XRD pattern reveals that the Fe and FeCo nanoparticles are stable in the acidic electrolyte. The stability of the metal nanoparticles might be due to a thin layer of carbonaceous coating when the PVP polymers were carbonized at 900 °C.

The BET surface area, BJH pore volume and elemental composition of the catalysts are also summarized in Table 1. The specific surface areas and pore volumes of the catalysts were slightly reduced which might be due to the formation of metal–nitrogen–carbon sites on the exteriors of carbon nanotubes. The actual metallic weight loadings of the annealed catalysts were lower than the nominal weight loadings.

The oxygen reduction activities of PVP–MWCNT-based NPMCs were assessed using rotating disc electrode (RDE) method [27]. A series of RDE curves of different catalysts measured in O_2-saturated 0.5 M H_2SO_4 at a sweep rate of 10 mV s^{-1} and rotation of 1000 rpm are shown in Fig. 5a. The onset potential is defined as the potential at which the ORR current is 5% of the diffusion-limited current [11]. The half-wave potential is defined as the halfway between the limiting current (measured as 0.1 V vs RHE) and zero current on the ORR voltammogram curve. The onset potential and half-wave potential of each catalyst are summarized in Table 2. The ORR performances of MWCNT–PVP, MWCNT–Fe and MWCNT–Co catalysts are very similar to each other, with onset potential and half-wave potential values of ~0.67 V and 0.46 V (vs RHE) respectively. A significant improvement in the ORR performance is

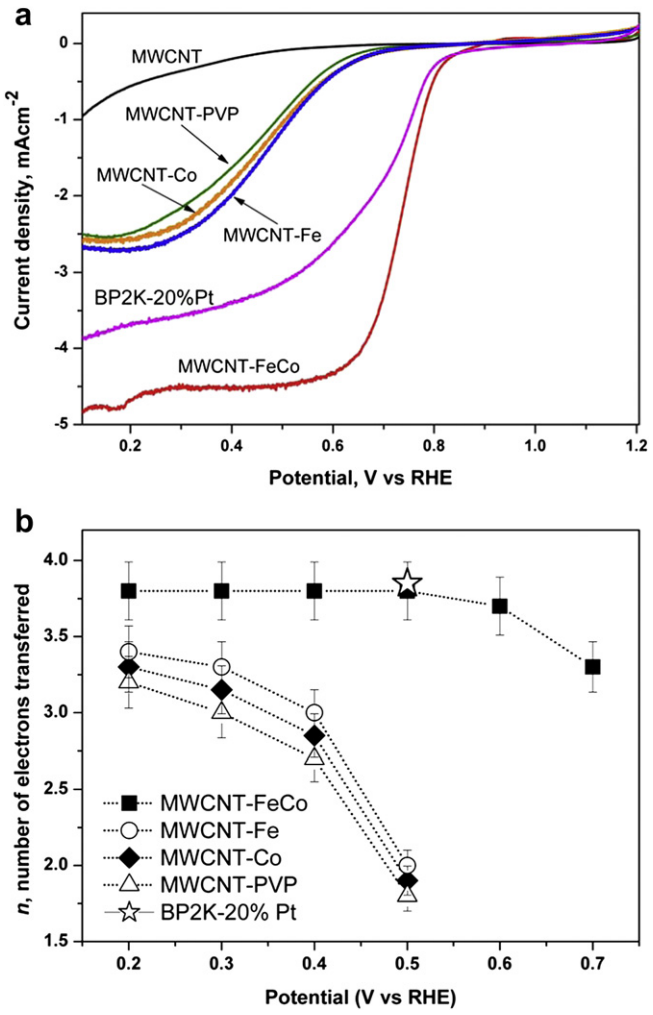

Fig. 5. (a) Rotating disk voltammograms for oxygen reduction of the non-precious metal–carbon nanotube catalysts modified glassy carbon electrodes in O_2-saturated 0.5 M H_2SO_4 at a sweep rate of 10 mV s^{-1} and 1000 rpm. (b) Plots of potential dependence of the number of electrons transferred per O_2 molecule based on Koutecky–Levich equation.

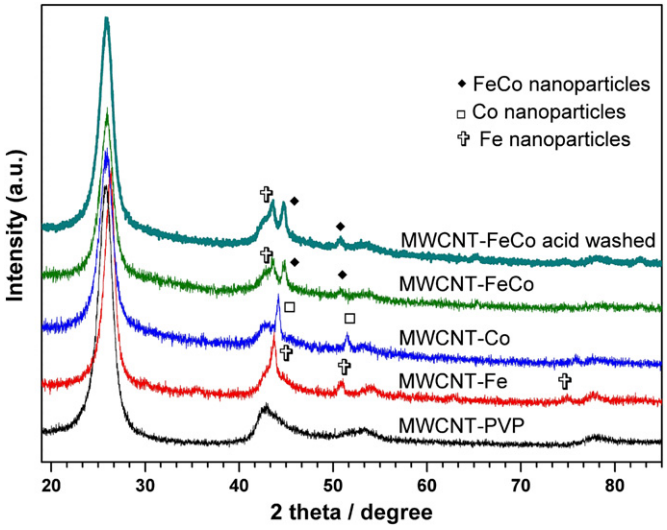

Fig. 4. X-ray diffraction (XRD) patterns of various non-precious metal–carbon nanotube-based catalysts.

observed for MWCNT–FeCo catalysts with onset potential and half-wave potential values of ~0.82 V and 0.73 V (vs RHE) respectively. The onset potential and half-wave potential values of BP2K-20%Pt are ~0.80 V and 0.70 V (vs RHE) respectively. The ORR performance of MWCNT–FeCo catalysts is comparable to the BP2K-20%Pt catalysts. The higher current density of MWCNT–FeCo is mainly due to the excellent electrical conductivity of carbon nanotubes compared to Black Pearl 2000 carbon. The excellent ORR performance of MWCNT–FeCo catalysts is attributed to the presence of

Table 2
Oxygen reduction reaction of non-precious metal–MWCNT-based catalysts.

Sample	Half-wave potential (vs RHE)	Onset potential (vs RHE)	n[a]
Pristine MWCNT	0.24	0.56	–
MWCNT–PVP	0.45	0.66	1.8
MWCNT–Fe	0.48	0.67	2.0
MWCNT–Co	0.47	0.67	1.9
MWCNT–FeCo	0.73	0.82	3.7
BP2K-20%Pt	0.70	0.80	3.8

[a] n is the number of electrons transferred per O_2 molecule as evaluated using the Koutecky–Levich equation at 0.5 V (vs RHE).

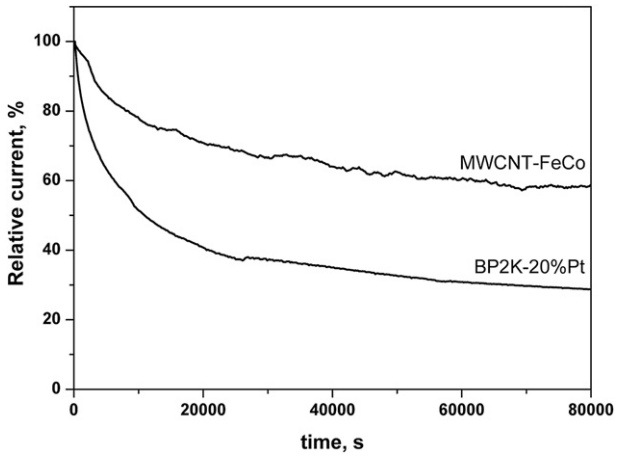

Fig. 6. Chronoamperometric response of MWCNT–FeCO and BP2K-20%Pt catalysts modified glassy carbon electrodes at 0.5 V in O_2-saturated 0.5 M H_2SO_4 at a rotation rate of 1000 rpm.

the bimetallic FeCo nanoparticles which might take part in the oxygen reduction reaction.

To better understand the ORR performance of the catalysts over the potential range studied, we evaluate the number of electrons transferred per O_2 molecule (n) involved in the oxygen reduction by using the Koutecky–Levich Eq. (1):

$$\frac{1}{i} = \frac{1}{i_k} + \frac{1}{i_d} = \frac{1}{nFAkC_{O_2}} + \frac{1}{0.62nFAD_{O_2}^{2/3}\nu^{-1/6}C_{O_2}\omega^{1/2}} \quad (1)$$

where i is the measured current, i_k and i_d are the kinetic and diffusion-limited currents respectively, k is the electrochemical rate constant for O_2 reduction, F is the faraday constant, D_{O_2} is the diffusion coefficient of O_2 in solution (1.4×10^{-5} cm^2 s^{-1}), C_{O_2} is the concentration of O_2 in solution (1.1×10^{-6} mol cm^{-3}), ν is the kinetic viscosity (0.01 cm^2 s^{-1}), A is the geometric area of the electrode (0.20 cm^2), and ω is the angular frequency of rotation in terms of rad s^{-1} for 0.5 M H_2SO_4 electrolyte [1]. All the parameters are invariant over the potential range with the exception of n values. A linear plot of i^{-1} versus $\omega^{-1/2}$ can be used to determine n value at a particular potential. In Fig. 5b the Loutecky–Levich plots are displayed over the potential range (0.7–0.2 V vs RHE), which were derived based on the ORR curves of the catalysts obtained at various rotating speeds (from 250 to 4000 rpm) at each particular potential. For the BP2K-20%Pt catalysts, the n value is determined to be ~3.8 at 0.5 V (vs RHE). The MWCNT–FeCo catalyst already exhibits ORR activity whereas other catalysts do not at 0.7 V (vs RHE). The n value of MWCNT–FeCo catalysts approaches ~3.7 at 0.5 V (vs RHE), while the n values of other non-precious catalysts are close to ~2. This result suggests that MWCNT–FeCo catalysts give rise to a four-electron transfer in oxygen reduction reaction at a much lower overpotential.

The long-term stability of catalysts is one of the major concerns in current PEM fuel cell technology. The stability of MWCNT–FeCo and BP2K-20%Pt catalysts was tested at a constant voltage of 0.5 V (vs RHE) for 80,000 s in a 0.5 M H_2SO_4 electrolyte saturated with O_2 at a rotation rate of 1000 rpm (see Fig. 6). The chronoamperometric response of MWCNT–FeCo retained a higher relative current of ~58% compared to BP2K-20%Pt which showed a relative current of ~29% after 80,000 s operation. This result indicates that the long-term stability of MWCNT–FeCo is better than BP2K-20%Pt catalyst.

The incorporation of binary Fe–Co metals as NPMCs has been reported in literature to yield better ORR activity than NPMCs based on single metal precursor [17–21]. Wu et al. [17] reported high performance NPMCs based on pyrolyzed polyaniline/FeCo. Choi et al. [21] synthesized binary FeCo-based NPMCs using ethylenediamine as nitrogen source and Ketjen Black as supports. The pyrolysis of binary metal tetraphenyl porphyrins (TPP) has also been investigated as NPMCs for improved ORR activity [21]. The pyrolyzed CoTPP/FeTPP yielded the best performing NPMCs and the catalytic sites were attributed to the formation of metal–N_4 cores. The Co–N_4 and Fe–N_4 cores were hypothesized to form a face-to-face bimetal structure with a specified stereo distance, which could provide facile reduction of oxygen to water. Thus the presence of binary FeCo alloys enhances the formation of catalytic active nitrogen dopants which subsequently contribute to the improvement of the ORR performance.

4. Conclusion

Non-precious metal catalysts were synthesized by using PVP–wrapped MWCNTs complexes with iron or/and cobalt ions. After annealing in 10% ammonia at 900 °C for 1 h, MWCNT–FeCo catalysts exhibited the highest electrochemical activity for ORR. The total metal and nitrogen loadings of MWCNT–FeCo were both ~1 wt.%. The onset potential and half-wave potential of MWCNT–FeCo catalysts were ~0.84 V and 0.76 V (vs RHE) respectively. MWCNT–FeCo catalysts exhibited n ~3.8 number of electrons transferred per O_2 molecule involved in the oxygen reduction. The MWCNT–FeCo catalysts also exhibit excellent long-term stability test.

References

[1] J. Zhang, PEM Fuel Cell Electrocatalysts and Catalyst Layers – Fundamental and Applications, Springer, 2008.
[2] B. Smitha, S. Sridhar, A.A. Khan, J. Membr. Sci. 259 (2005) 10–26.
[3] R. Devanathan, Energy Environ. Sci. 1 (2008) 101–119.
[4] T. Matsumoto, T. Komatsu, K. Arai, T. Yamazaki, M. Kijima, H. Shimizu, Y. Takasawa, J. Nakamura, Chem. Commun. 7 (2004) 840–841.
[5] D.M. Bernardi, M.W. Verbrugge, J. Electrochem. Soc. 139 (1992) 2477–2491.
[6] L. Zhang, J. Zhang, D.P. Wilkinson, H. Wang, J. Power Sources 156 (2006) 171–182.
[7] C.W.B. Bezerra, L. Zhang, K. Lee, H. Liu, A.L.B. Marques, E.P. Marques, H. Wang, J. Zhang, Electrochim. Acta 53 (2008) 4937–4951.
[8] B.N. Popov, X. Li, G. Liu, J. Lee, Int. J. Hydrogen Energy 36 (2011) 1794–1802.
[9] A.A. Gewirth, M.S. Thorum, Inorg. Chem. 49 (2010) 3557–3566.
[10] Y. Nabae, S. Moriya, K. Matsubayashi, S.M. Lyth, M. Malon, L. Wu, N.M. Islam, Y. Koshigoe, S. Kuroki, M. Kakimoto, S. Miyata, J. Ozaki, Carbon 48 (2010) 2613–2624.
[11] L. Birry, J.H. Zagal, J. Dodelet, Electrochem. Commun. 12 (2010) 628–631.
[12] M. Lefevre, J. Dodelet, P. Bertrand, J. Phys. Chem. B 106 (2002) 8705–8713.
[13] H. Kalvelage, A. Mecklenburg, U. Kunz, U. Hoffmann, Chem. Eng. Technol. 23 (2009) 803–807.
[14] M. Yuasa, A. Yamaguchi, H. Itsuki, K. Tanaka, M. Yamamoto, K. Oyaizu, Chem. Mater. 17 (2005) 4278–4281.
[15] V. Nallathambi, N. Leonard, R. Kothandaraman, S.C. Barton, Electrochem. Solid-State Lett. 14 (2011) B55–B58.
[16] R. Liu, D. Wu, X. Feng, K. Mullen, Angew. Chem. Int. Ed. 49 (2010) 2565–2569.
[17] G. Wu, K.L. More, C.M. Johnston, P. Zelenay, Science 332 (2011) 443–447.
[18] V. Bambagioni, C. Bianchini, J. Filippi, A. Lavacchi, W. Oberhauser, A. Marchionni, S. Moneti, F. Vizza, R. Psaro, V. Dal Santo, A. Gallo, S. Recchia, L. Sordelli, J. Power Sources 196 (2011) 2519–2529.
[19] S. Li, L. Zhang, J. Kim, M. Pan, Z. Shi, J. Zhang, Electrochim. Acta 55 (2010) 7346–7353.
[20] D. Chu, R. Jiang, Solid State Ionics 148 (2002) 591–599.
[21] J.Y. Choi, R.S. Hsu, Z. Chen, J. Phys. Chem. C 114 (2010) 8048–8053.
[22] M.J. O'Connell, P. Boul, L.M. Ericson, C. Huffman, Y.H. Wang, E. Haroz, C. Kuper, J. Tour, K.D. Ausman, R.E. Smalley, Chem. Phys. Lett. 342 (2001) 265–271.
[23] F. Bonet, K. Tekaia-Elhsissen, K.V. Sarathy, Bull. Mater. Sci. 23 (2000) 165–168.
[24] H.A. Maturana, I.M. Peric, S.A. Pooley, B.L. Rivas, Polym. Bull. 45 (2000) 425–429.
[25] N. Tokman, S. Akman, C. Ozeroglu, Talanta 63 (2004) 699–703.
[26] J.R. Pels, F. Kapteijin, J.A. Moulijn, Q. Zhu, K.M. Thomas, Carbon 33 (1995) 1641–1653.
[27] K.J.J. Mayrhofer, D. Strmcnik, B.B. Blizanac, V. Stamenkovic, M. Arenz, N.M. Markovic, Electrochim. Acta 53 (2008) 3181–3188.